Available online at www.sciencedirect.com
SCIENCE DIRECT®
Journal of Photochemistry and Photobiology A: Chemistry 166 (2004) 107–113
Journal of Photochemistry and Photobiology A:Chemistry
www.elsevier.com/locate/jphotochem

A nano-modified Si/TiO_2 composite electrode for efficient solar water splitting

Susumu Takabayashi [a], Ryuhei Nakamura [a], Yoshihiro Nakato [a,b,*]

[a] *Division of Chemistry, Graduate School of Engineering Science, Osaka University, Toyonaka, Osaka 560-8531, Japan*
[b] *Core Research for Evolutional Science and Technology (CREST), Japan Science and Technology Agency (JST), Kawaguchi Center Building, Kawaguchi, Saitama 332-0012, Japan*

Received 13 November 2003; received in revised form 9 January 2004; accepted 5 April 2004

Abstract

Solar water splitting with a composite polycrystalline-Si/doped TiO_2 thin-film electrode is proposed as a promising new approach to high-efficiency and low-cost solar-to-chemical conversion. The advantage, efficiency, stability, and some problems to be solved are reviewed mainly on the basis of reported results. It is shown that (1) an n-Si electrode with surface alkylation and metal nano-dot coating gives an efficient and stable photovoltaic characteristic, (2) TiO_2 (and similar metal oxides) doped with other elements, such as nitrogen and sulfur, can cause water photooxidation (oxygen photoevolution) by visible-light illumination, and thus (3) a coupling of these two electrodes is effective for efficient water splitting under solar illumination.
© 2004 Elsevier B.V. All rights reserved.

Keywords: Hydrogen; Photoelectrochemistry; Photocatalysis; Thin film; Nano-particles; Surface modification

1. Introduction

The main target in recent studies on solar energy conversion is to achieve enough lowering of the fabrication cost without lowering the conversion efficiency. Much attention has thus been paid to thin-film solar cells [1], fabricated by use of inexpensive thin-film semiconductor materials, such as amorphous silicon (a-Si), polycrystalline Si, and particulate TiO_2 with a photosensitizing dye. However, unfortunately, the thin-film solar cells have a serious disadvantage in that it is inevitably necessary to use films of expensive transparent conductive oxide (TCO), such as indium tin oxide (ITO), for efficient photocurrent collection. In addition, the TCO film has actually no enough electrical conductivity, and thus we have to adopt a complicated solar-cell structure, composed of a large number of small cells connected in series, in order to avoid an increase in ohmic loss. This also leads to an increase in the fabrication cost.

In this respect, solar-to-chemical conversion by use of a semiconductor/electrolyte junction, such as solar water splitting, is very promising because in this method, no photocurrent collection is necessary and thus no transparent conductive oxide is necessary. This method has in principle a strong merit in the cost lowering. However, the solar water splitting with a semiconductor electrode is not an easy task. A large number of studies have been made on this subject since the pioneering work by Fujishima and Honda [2], but the conversion efficiency reported still remains quite low (<1%) if we separate high efficiencies reported for high-quality, expensive, multi-layered single-crystal semiconductor electrodes such as AlGaAs/Si [3] and $GaInP_2$/GaAs [4].

In the present paper, we propose a new approach to the high-efficiency and low-cost solar energy conversion by use of a composite polycrystalline-Si/doped TiO_2 thin-film electrode, such as shown in Fig. 1. At present, we have not yet constructed the composite Si/TiO_2 electrode itself, but a simple calculation based on the characteristics of individual Si and doped TiO_2 electrodes has shown that this composite electrode will be able to yield a high conversion efficiency of more than 10%. It should be noted also that the composite Si/TiO_2 electrode is composed of inexpensive thin-film semiconductor materials. In the following sections, we will explain the present stage of our studies on this approach, together with some problems involved there.

* Corresponding author. Tel.: +81-6-6850-6235; fax: +81-6-6850-6236.
E-mail address: nakato@chem.es.osaka-u.ac.jp (Y. Nakato).

1010-6030/$ – see front matter © 2004 Elsevier B.V. All rights reserved.
doi:10.1016/j.jphotochem.2004.04.037

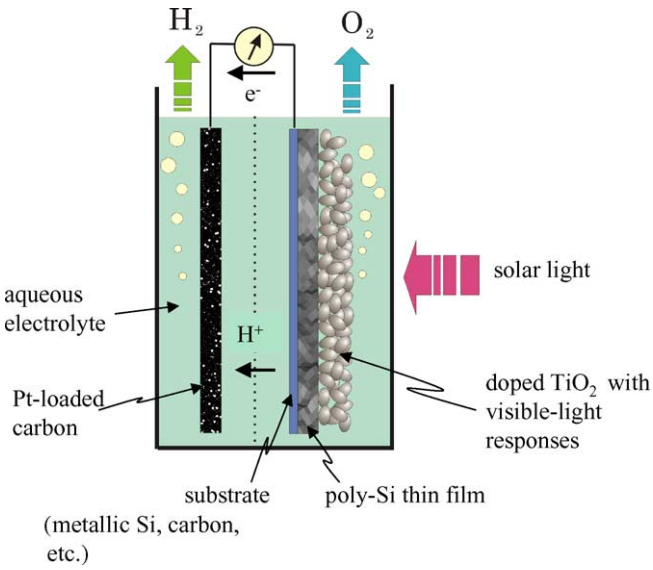

Fig. 1. Schematic illustration of solar water splitting with a composite polycrystalline-Si/doped TiO_2 semiconductor electrode.

2. Operation principle of the composite Si/TiO_2 electrode

Fig. 2 shows the operation principle of the composite polycrystalline-Si/doped TiO_2 thin-film electrode (Fig. 1). It is well known [1] that TiO_2 is chemically stable and can photooxidize water into oxygen and H^+ ions but only absorbs UV light below about 420 nm. Recently, however, it was reported by several workers [5–10] that doping of TiO_2 with N, C, S or other elements caused photo-responses in the visible-light region. A similar effect was reported for other metal oxides such as Ta_2O_5 [11,12]. Moreover, oxygen evolution was really observed for powdered photocatalyst systems under visible light illumination [7,11,12], though only in the presence of an oxidant as a sacrificial reagent.

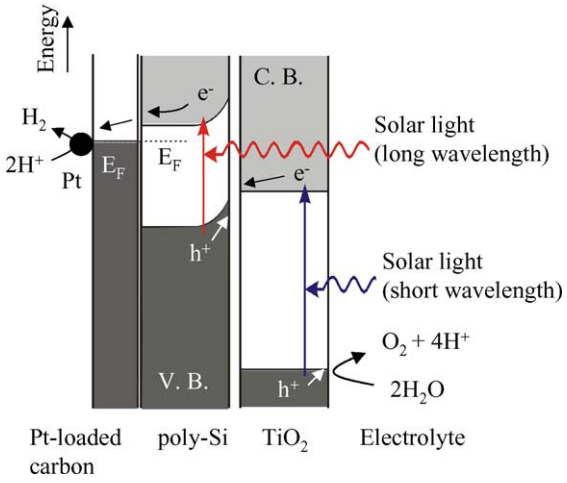

Fig. 2. The operation principle of the composite polycrystalline-Si/doped TiO_2 thin-film electrode of Fig. 1.

Thus, the doped TiO_2 can be used for water photooxidation by a short-wavelength part of solar light (blue light), in the composite electrode of Fig. 1. The long-wavelength part of the solar light (red light) that is not absorbed by the doped TiO_2, on the other hand, passes through it and is absorbed by a backside polycrystalline-Si layer. Accordingly, an electron is excited stepwise from a low level (of the valence band of TiO_2) to a high level (of the conduction band of Si), which leads to efficient hydrogen evolution on the counter-electrode and efficient oxygen evolution on the doped TiO_2 surface. We can say that the composite Si/TiO_2 electrode effectively utilizes the wide distribution of the solar spectrum for efficient solar water splitting.

The solar-to-chemical energy conversion efficiency, ϕ^{S}_{chem}, can be calculated by the following equation:

$$\phi^{S}_{chem} = \left[\frac{(\Delta G/e) \times j}{\text{input solar energy}}\right] \times 100\,(\%) \quad (1)$$

where ΔG is the Gibbs energy change for water splitting, which equals 1.23 eV under the standard conditions at 298 K, e the elementary charge, and j the photocurrent density observed.

A simple calculation by use of Eq. (1) shows that it is not difficult to get a high conversion efficiency of 10% in the composite Si/TiO_2 electrode. For example, if we observe a photocurrent density of 10 mA cm^{-2} under solar illumination of 100 mW cm^{-2}, the ϕ^{S}_{chem} value reaches $(1.23 \times 10/100) \times 100 = 12.3\,(\%)$. From the solar spectrum, we can expect that doped TiO_2 that absorbs the solar light in wavelengths (λ) shorter than 500 nm yields a photocurrent density of about 10 mA cm^{-2}. The underlying polycrystalline Si can yield a higher photocurrent density of about 30 mA cm^{-2} by the solar light in $\lambda \geq 500$ nm. As it is not difficult to find doped TiO_2 that absorbs light in $\lambda \leq 500$ nm, these considerations indicate that the composite Si/TiO_2 electrode can yield a conversion efficiency of more than 10%.

3. Photoelectrochemical characteristics of surface-methylated and Pt nano-dotted n-Si

Although the composite Si/TiO_2 electrode can in principle yield a high conversion efficiency, as mentioned above, we have still some problems to be solved in order to achieve such a high efficiency in an actual system. They may be listed in the following: (1) the generation of a high photovoltage at the Si/electrolyte interface; (2) the stabilization of Si in aqueous electrolytes; (3) the regulation of the flat-band potential of n-Si and the energy level matching at the Si/TiO_2 interface; (4) the preparation of doped TiO_2 that can cause efficient visible-light oxygen photoevolution.

Let us first consider the generation of a high photovoltage at the Si/electrolyte interface. Fortunately, we can solve this problem on the basis of our previous studies. We reported before [13–20] that single-crystal n-Si electrodes coated with metal nano-particles, in contact with a redox elec-

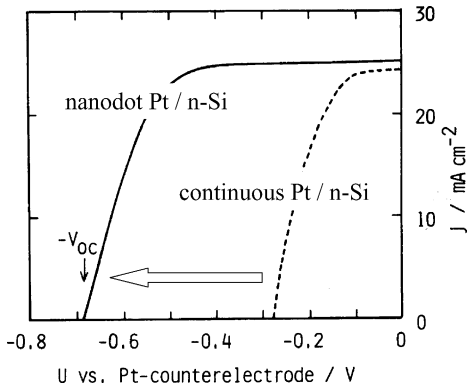

Fig. 3. Photocurrent density (j) vs. potential (U) for a Pt nano-dotted n-Si (1 1 1) electrode in 8.6 M HBr + 0.05 M Br_2, compared with that for an n-Si electrode coated with a continuous Pt layer.

trolyte, generated very high open-circuit photovoltages (V_{oc}) of 0.62–0.64 V, considerably higher than those (0.59 V) of conventional solid-state p–n junction Si solar cells of a similar simple structure. Fig. 3 shows an example of photocurrent density (j) versus potential (U) characteristics observed for a Pt nano-dotted n-Si (1 1 1) electrode in 8.6 M HBr + 0.05 M Br_2, compared with that for an n-Si electrode coated with a continuous Pt layer. It is to be noted that the V_{oc} for the former electrode is very high. This remarkable result is entirely due to the effect of metal nano-dot coating [14,15]. Quantitative analyses, using n-Si electrodes with well-regulated distributions of Pt particles, prepared by use of their Langmuir–Blodgett layers, have shown [18] that *ideal* minority-carrier-controlled solar cells can be fabricated by this method. It should be emphasized also that the method can be applied easily to inexpensive polycrystalline Si thin films.

The problem remaining in the Si electrode was that it gradually degraded owing to surface oxidation in aqueous electrolytes under illumination and showed no enough stability for long-term operation. Recently, we have found [21,22] that this problem can be solved by surface alkylation. The modification of Si surfaces with organic alkyl groups has recently attracted growing attention in various respects [23–34]. As to the Si stabilization, it was reported that the surface alkylation improved the Si stability against surface oxidation in air [31] and in an aqueous redox electrolyte [32]. However, it was also reported [33,34] that the surface alkylation tended to retard interfacial electron transfer at the Si/redox electrolyte interface. We have found that this dilemma can be solved by a combination of surface alkylation and metal nano-dot coating, because in this case the metal nano-dots can act as a catalyst for interfacial electron transfer reactions [14,15].

Fig. 4 shows a result of a photocurrent stability test for various n-Si electrodes in 8.6 M HBr+0.05 M Br_2 at 25 °C. The photocurrent for naked (H-terminated) n-Si decays quickly because it is readily oxidized at the surface under these conditions. The photocurrent for the H-terminated n-Si can be

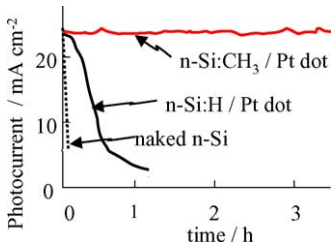

Fig. 4. Photocurrent vs. time for naked (H-terminated) n-Si, Pt nano-dotted n-Si, and surface-methylated and Pt nano-dotted n-Si in 8.6 M HBr + 0.05 M Br_2 at 25 °C.

stabilized to some extent by coating with Pt nano-dots, but still decays in a time range of 10–20 min. On the other hand, the photocurrent for surface-methylated (CH_3-terminated) and Pt nano-dotted n-Si is kept stable for a long time of more than 3 h. We have to note that the surface-methylated and Pt-dotted electrode is stabilized even in a highly corrosive electrolyte of 8.6 M HBr + 0.05 M Br_2.

The surface methylation (CH_3-termination) in the present work was obtained by the method of Lewis and coworkers [25]. The chemical procedures are shown in Fig. 5. HF- and NH_4F-etched and hence H-terminated n-Si (1 1 1) was refluxed in a chlorobenzene solution of PCl_5 under UV illumination, followed by reflux in an ether solution of CH_3MgBr (Grignard reagent). The Pt particles were deposited electrochemically at −1.0 V versus Ag/AgCl in a solution of 5 mM K_2PtCl_6 + 100 mM $LiClO_4$. The electricity passing across the electrode surface was 83 mC cm^{-2}. The Pt deposition on the surface-methylated n-Si gave a current density versus potential curve similar to that on the H-terminated n-Si, suggesting that Pt for the surface-methylated n-Si was deposited on non-methylated (uncovered) parts of the Si surface, as shown in Fig. 5.

The occurrence of surface methylation was confirmed by XPS analysis [21]. The surface-methylated (CH_3-terminated) Si surface gave the carbon-1s XPS peak at 283.8 eV, attributable to carbon in surface Si–CH_3 bonds [29,35], in contrast to non-methylated (H-terminated) Si surfaces. A very rough estimation of the surface coverage (θ) of CH_3 group from the C and Si XPS peaks, using the method of Himpsel et al. [36], gave a value of around 70%, which was somewhat higher than a reported value

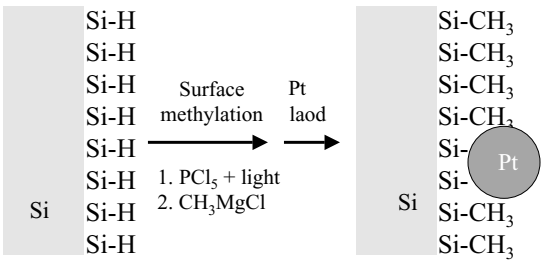

Fig. 5. Chemical procedures for surface methylation and Pt nano-dot coating.

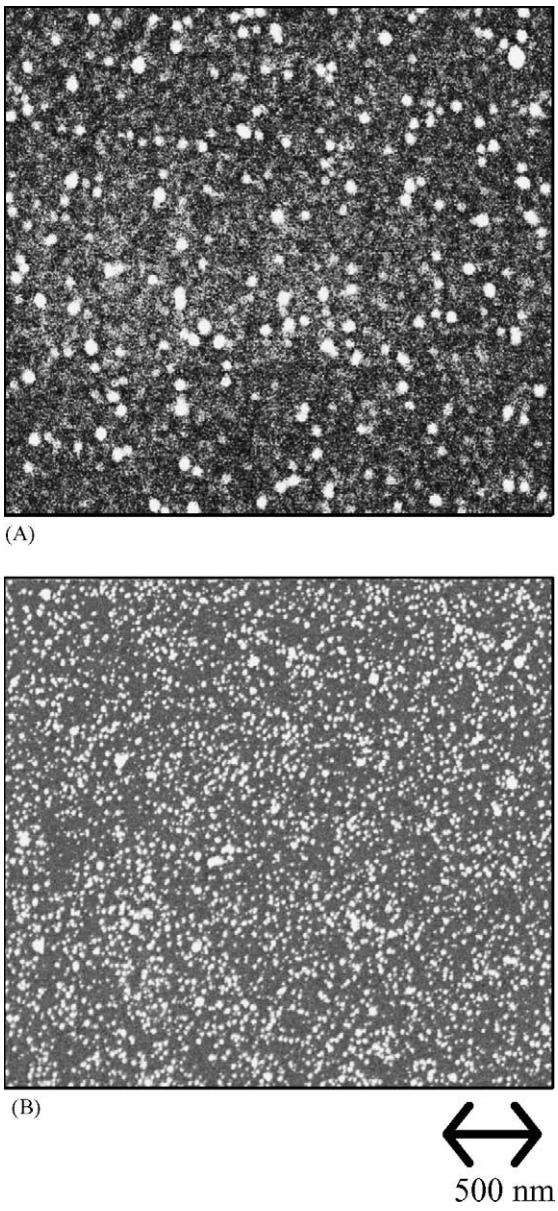

Fig. 6. Scanning electron micrographs (SEMs) of (A) surface-methylated (CH_3-terminated) and Pt nano-dotted and (B) H-terminated and Pt nano-dotted n-Si surfaces just after Pt deposition.

of less than 50% [28] probably owing to an influence of contaminating organic compounds at the Si surface.

Fig. 6 shows scanning electron micrographs (SEMs) of (A) surface-methylated (CH_3-terminated) and Pt nano-dotted and (B) H-terminated and Pt nano-dotted n-Si surfaces just after Pt deposition. Circular Pt particles were deposited fairly homogeneously all over the n-Si surface in both cases, though the size and density of the Pt particles were rather different between the CH_3-terminated and the H-terminated n-Si.

Fig. 7 shows photocurrent density (j) versus potential (U) curves for a surface-methylated (CH_3-terminated) and Pt nano-dotted n-Si (1 1 1) electrode in 7.6 M HI+0.05 M I_2 under simulated solar illumination (AM1.5G, 100 mW cm^{-2}),

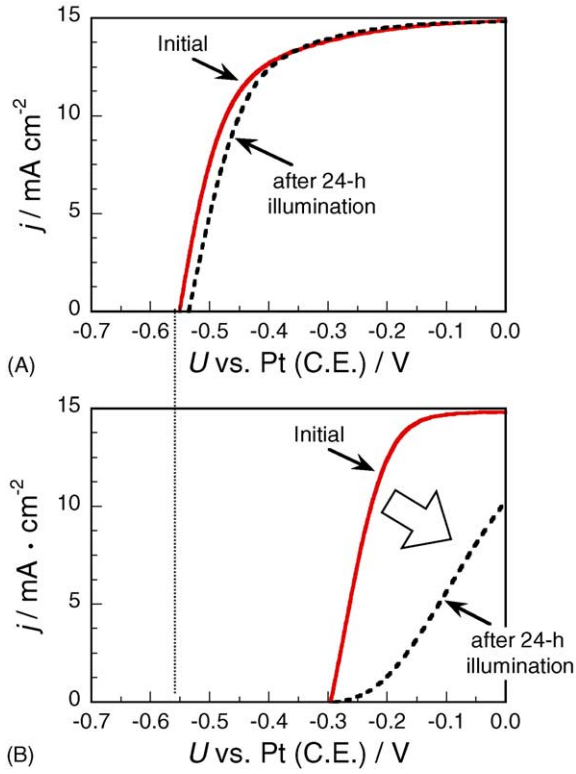

Fig. 7. Photocurrent density (j) vs. potential (U) for (A) surface-methylated (CH_3-terminated) and Pt nano-dotted and (B) H-terminated and Pt nano-dotted n-Si in 7.6 M HI + 0.05 M I_2 under simulated solar illumination (AM1.5G, 100 mW cm^{-2}).

compared with those for H-terminated and Pt nano-dotted n-Si (1 1 1). Solid curves were observed at the initial stage of illumination, whereas dotted curves were observed after 24 h illumination. It should be noted that the surface-methylated n-Si (1 1 1) gives high V_{oc} as well as high stability, compared with the H-terminated n-Si (1 1 1), clearly indicating the effectiveness of the surface methylation. A slight decrease in the V_{oc} for the surface-methylated and Pt-dotted n-Si (1 1 1) after the 24 h illumination is not due to the degradation of the n-Si electrode but an increase in the concentration of I_2 (or I_3^-) as an oxidant of the redox couple in the electrolyte.

Fig. 8 shows Si 2p XPS peaks for (A) surface-methylated (CH_3-terminated) and Pt-dotted and (B) H-terminated and Pt-dotted n-Si surfaces. Similar to Fig. 7, solid curves were observed at the initial stage of illumination, whereas dotted curves were observed after 24 h illumination. The H-terminated and Pt-dotted n-Si showed an additional high-energy peak at 103.5 eV, attributed to formation of SiO_2 (Fig. 6B), suggesting that the H-terminated n-Si(1 1 1) surface was slightly oxidized during the Pt deposition. It is likely that the large positive shift of the onset potential of the photocurrent (or the large decrease in the V_{oc}) for the H-terminated and Pt-dotted n-Si in Fig. 7, compared with the surface-methylated and Pt-dotted n-Si, is caused by the surface oxidation, which will induce a positive shift in the flat-band potential (U_{fb}) of n-Si owing to an electrical

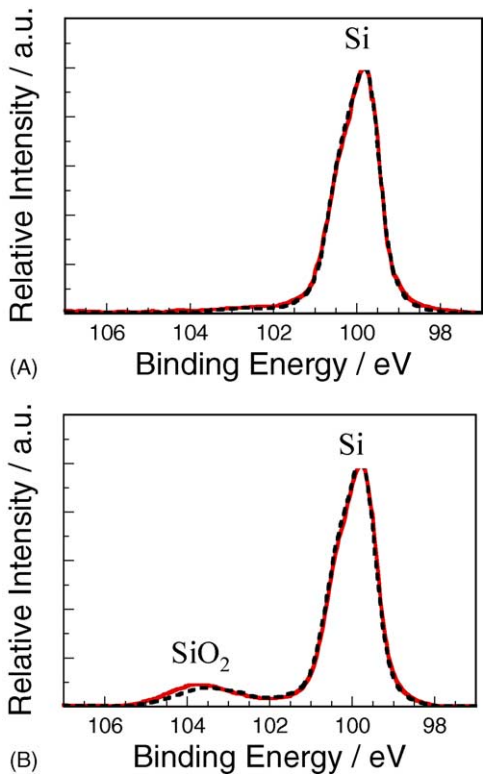

Fig. 8. Si 2p XPS peaks for (A) surface-methylated (CH_3-terminated) and Pt-dotted and (B) H-terminated and Pt-dotted n-Si surfaces.

double layer of surface dipoles ($Si^{\delta+}$–$O^{\delta-}$). The stabilization of n-Si by the surface methylation might be explained to be due to the formation of a hydrophobic thin layer on the Si surface, which will prevent the contact of water molecules to the Si surface.

4. Efficient solar to chemical conversion through photodecomposition of HI with n-Si

The surface-methylated and Pt nano-dotted n-Si electrode gives a high V_{oc} in 7.6 M HI (Fig. 7) and can thus be used for efficient solar decomposition of hydrogen iodide (HI) into hydrogen (H_2) and iodine (I_2 or I_3^-). The important point is that the anodic current for the methylated and Pt-dotted n-Si electrode in Fig. 7, corresponding to the oxidation of I^- to I_2 or I_3^-, starts to flow at a potential considerably more negative than the cathodic current (not shown in Fig. 7) on Pt, corresponding to hydrogen evolution. This implies that the solar decomposition of HI into H_2 and I_2 (or I_3^-) occurs in a photoelectrochemical cell such as shown in Fig. 9 spontaneously with no external bias.

The decomposition of HI into H_2 and I_2 (or I_3^-) is an up-hill reaction with the standard Gibbs energy change $\Delta G^\circ = 0.54$ eV. Thus, the solar decomposition of HI into H_2 and I_2 in a cell of Fig. 9 implies that the solar energy is converted to chemical energy, similar to the case of water splitting. Actually, the obtained H_2 and I_2 (or I_3^-) can be

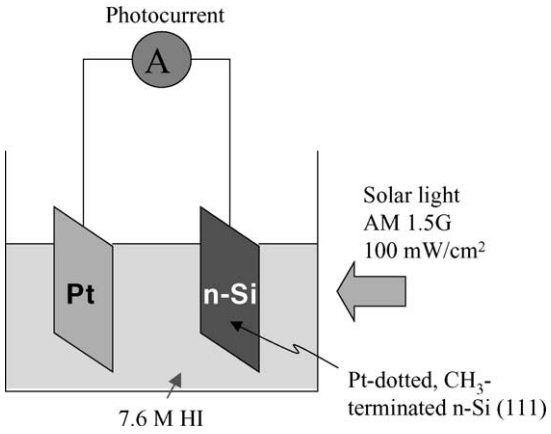

Fig. 9. Schematic illustration of a photoelectrochemical cell for solar decomposition of HI into H_2 and I_2 (or I_3^-).

regarded as a fuel, and used to generate an electric power by constructing a kind of fuel cell.

The solar to chemical conversion efficiency, ϕ^{S}_{chem}, can be calculated by Eq. (1). We investigated experimentally various cell parameters, such as the redox potential for the I^- oxidation, $E(I_3^-/I^-)$, and that for the hydrogen evolution, $E(H^+/H_2)$, the Gibbs energy change ΔG $[=e\{E(I_3^-/I^-)-E(H^+/H_2)\}]$, and the photocurrent density, j, as a function of the HI concentration. The $E(I_3^-/I^-)$ and $E(H^+/H_2)$ values were obtained by measuring current–potential curves with a Pt electrode in given electrolytes. These studies showed that ΔG decreases, whereas j increases, with the increasing HI concentration. The ϕ^{S}_{chem} value thus became a maximum at the HI concentration of 3.2–4.5 M, yielding a value of 7.4% [22]. This value is probably the highest for the solar to chemical conversion efficiencies ever reported, if we separate the high values reported for the expensive, high-quality, composite multi-layer semiconductor electrodes such as p–n $Al_xGa_{1-x}As$/p–n Si [3] and p–n GaAs/p-$Ga_xIn_{1-x}P$/Pt [4].

5. Photoelectrochemical characteristics of doped TiO_2

The important target in this work is to develop doped TiO_2 that can cause efficient visible-light oxygen evolution. We confirmed that thin-film electrodes of TiO_2 doped with N, C or other elements had an ability to generate photocurrents under visible-light illumination in aqueous electrolyte solutions.

Fig. 10 shows, as an example, the incident photon to current efficiency (IPCE) versus wavelength for an N-doped TiO_2 [5,6] film, prepared on a commercial conductive oxide layer. The photocurrent was measured in 0.05 M H_2SO_4. The N-doped TiO_2 was in the present work synthesized by adding 28% aqueous ammonia to Ti(*i*-$OC_3H_7)_4$ at 0 °C, followed by heating at 400 °C for 6 h. The IPCE indeed extends to about 550 nm, but the IPCE values in the visible-light region are very low. Fig. 11 shows another example of the

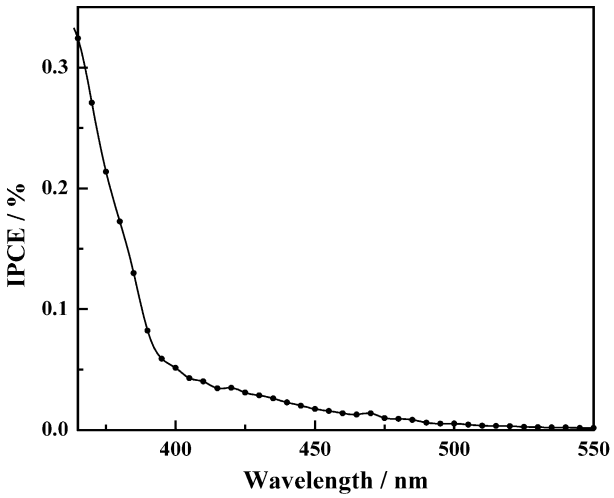

Fig. 10. The incident photon to current efficiency (IPCE) vs. wavelength in 0.05 M H_2SO_4 for an N-doped TiO_2 film, prepared by addition of $Ti(i\text{-}OC_3H_7)_4$ and 28% aqueous ammonia at 0 °C, followed by heating at 400 °C for 6 h.

IPCE versus wavelength for a TiO_2 film codoped with Cr and Sb, first reported by Kato and Kudo [7]. The Cr, Sb-codoped TiO_2 was in the present work prepared by sintering a mixture of TiO_2 (the standard sample of Catalysis Society of Japan, called TIO-3, rutile), Sb_2O_3 (1.25 mol%), and Cr_2O_3 (0.5 mol%) at 1150 °C for 10 h. The IPCE extends to about 550 nm, but the values in the visible-light region are very low, similar to the case of Fig. 10. The photocurrents will be attributed to oxygen evolution because the electrolyte solutions contained only indifferent (stable) salts. In fact, oxygen evolution was really observed for reported powdered photocatalysts with sacrificial reagents under visible light illumination [7,11,12], as mentioned earlier. Exploration of more efficient materials is now under way.

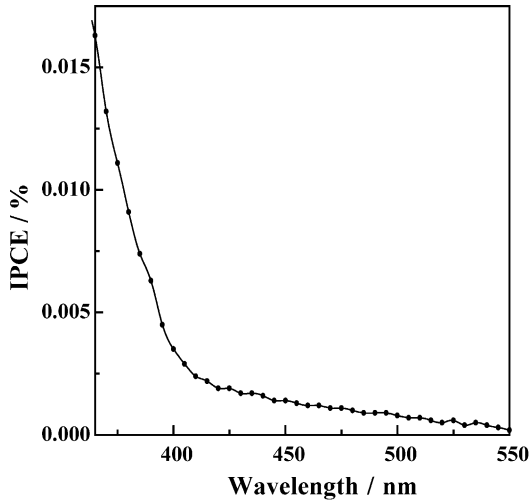

Fig. 11. The incident photon to current efficiency vs. wavelength in 0.05 M H_2SO_4 for a Cr, Sb-codoped TiO_2 film, prepared by annealing a mixture of TiO_2, Sb_2O_3 (1.25 mol%), and Cr_2O_3 (0.5 mol%) at 1150 °C for 10 h.

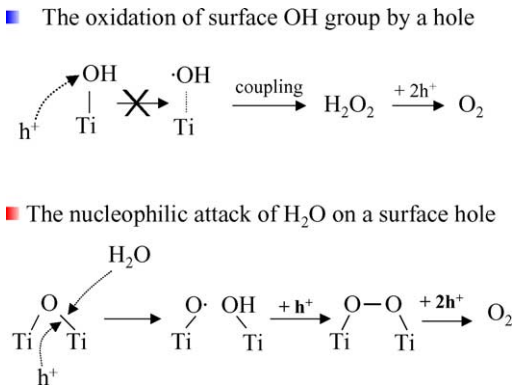

Fig. 12. New molecular mechanism for oxygen photoevolution on TiO_2 (rutile), elucidated by use of in situ photocurrent and PL measurements as well as in situ multiple internal reflection FTIR absorption spectroscopy.

As to the doped TiO_2 with efficient visible-light responses, we have another problem to be considered. We have to clarify whether the doped TiO_2 is active and stable enough, because we can expect that the doping will induce (1) a distortion in the TiO_2 crystal, (2) bond weakening, and (3) a decrease in the oxidation power of photogenerated holes. The third will be induced, for instance, by formation of some doping-induced surface states that trap the photogenerated holes, in the band gap. These problems can be solved by elucidation of molecular mechanism of oxygen photoevolution reaction on doped TiO_2. In this context, it may be interesting to note that we have recently succeeded in clarifying primary intermediates of oxygen photoevolution reaction on single-crystal n-TiO_2 (rutile) electrodes in aqueous electrolytes [37,38].

The main conclusion is that the oxygen photoevolution reaction is not initiated by the oxidation of surface OH group ($Ti\text{-}OH_s$) with photogenerated holes (h^+):

$$Ti\text{-}OH_s + h^+ \rightarrow [Ti \cdot OH]_s{}^+ \quad (2)$$

but by a nucleophilic attack of an H_2O molecule (Lewis base) to a surface-trapped hole (Lewis acid), accompanied by bond breaking:

$$[Ti\text{-}O\text{-}Ti]_s + h^+ + H_2O \rightarrow [Ti\text{-}O \cdot HO\text{-}Ti]_s + H^+ \quad (3)$$

It is worth noting that reaction (2) is an electron-transfer-type reaction, whereas reaction (3) is a Lewis acid–base-type reaction, and therefore their energetics and kinetics are quite different from each other. The conclusion is also shown in Fig. 12 more clearly. The conclusion was obtained by in situ spectroscopic studies such as photoluminescence (PL) and multiple internal reflection (MIR) infrared (IR) absorption measurements [37,38], in combination with in situ photocurrent measurements.

Such mechanistic studies can be extended to investigations of molecular mechanisms at the doped TiO_2 surface. It is quite an interesting subject to clarify how the mechanism at the TiO_2 surface is modified by doping with other elements. Deposition of RuO_2 nano-particles as an efficient

oxygen evolution catalyst on doped TiO_2 will be effective for its activation and stabilization, similarly to the case of n-Si-coated Pt nanoparticles [13–20].

The final problem is the regulation of the flat-band potential (U_{fb}) of n-Si and the energy level matching at the Si/TiO_2 interface. The highest conversion efficiency will be obtained when (1) upward band bending is formed in n-Si near the interface and (2) the top of the valence band of n-Si and the bottom of the conduction band of doped TiO_2 coincide with each other, just as shown in Fig. 2. It is to be noted here that, for a composite Si/TiO_2 electrode of Fig. 1, in which a porous particulate TiO_2 layer is deposited on n-Si, a major part of the Si surface is in contact with an aqueous electrolyte and thus the band energies of Si at the surface are determined mainly by the Si/electrolyte contact [14,15]. Based on this concept, studies on the regulation of the surface band energies of Si by modulation of interface potential are now in progress in our laboratory.

6. Conclusion

Solar water splitting with a composite polycrystalline-Si/doped TiO_2 thin-film electrode has a strong advantage over thin-film solar cells, in that there is no need to use expensive transparent conductive oxide such as indium tin oxide. A simple calculation has shown that a combination of inexpensive polycrystalline Si and particulate doped TiO_2 thin films can yield a high solar-to-chemical conversion efficiency of more than 10%. It is shown that the method of surface-methylation and metal nano-dot coating gives an efficient and stable Si electrode. On the other hand, further studies are necessary to find doped TiO_2 (or other metal oxides) that show much more efficient photocurrents in the visible light region. The elucidation of molecular mechanism of oxygen photoevolution on doped TiO_2 (or other metal oxides) with efficient visible-light responses is also necessary to confirm their high activity and stability. We can say that the solar water splitting with a composite Si/TiO_2 thin-film electrode will be one of the most promising approaches to efficient and low-cost solar energy conversion.

Acknowledgements

The authors would like to thank all co-workers in this research project for their kind co-operation, discussion, encouragement, and assistance.

References

[1] http://www.pv.unsw.edu.au/eff.
[2] A. Fujishima, K. Honda, Nature 238 (1972) 37.
[3] S. Licht, B. Wang, T. Soga, M. Umeno, Appl. Phys. Lett. 74 (1999) 4055.
[4] O. Khaselev, J.A. Turner, Science 280 (1998) 425;
O. Khaselev, J.A. Turner, Electrochem. Solid State Lett. 2 (1999) 310.
[5] S. Sato, Chem. Phys. Lett. 123 (1986) 126.
[6] R. Asahi, T. Morikawa, T. Ohwaki, K. Aoki, Y. Taga, Science 293 (2001) 269.
[7] H. Kato, A. Kudo, J. Phys. Chem. B 106 (2002) 5029.
[8] A. Zou, J. Ye, K. Sayama, H. Arakawa, Nature 414 (2001) 625.
[9] T. Ohno, T. Mitsui, M. Matsumura, Chem. Lett. 32 (2003) 364.
[10] H. Irie, Y. Watanabe, K. Hashimoto, Chem. Lett. 32 (2003) 772.
[11] G. Hitoki, T. Takata, J.N. Kondo, M. Hara, H. Kobayashi, K. Domen, Chem. Commun. (2002) 1698.
[12] A. Ishikawa, T. Takata, J.N. Kondo, M. Hara, H. Kobayashi, K. Domen, J. Am. Chem. Soc. 124 (2002) 13547.
[13] Y. Nakato, H. Yano, H. Tsubomura, Chem. Lett. (1986) 987.
[14] Y. Nakato, K. Ueda, H. Yano, H. Tsubomura, J. Phys. Chem. 92 (1988) 2316.
[15] Y. Nakato, H. Tsubomura, Electrochim. Acta 37 (1992) 897.
[16] S. Yae, I. Nakanishi, Y. Nakato, N. Toshima, H. Mori, J. Electrochem. Soc. 141 (1994) 3077.
[17] Y. Nakato, K. Kai, K. Kawabe, Sol. Energy Mater. Sol. Cells 37 (1995) 323.
[18] J.G. Jia, M. Fujitani, S. Yae, Y. Nakato, Electrochim. Acta 42 (1997) 431.
[19] K. Kawakami, T. Fujii, S. Yae, Y. Nakato, J. Phys. Chem. B 101 (1997) 4508.
[20] M. Ishida, K. Morisawa, R. Hinogami, J.G. Jia, S. Yae, Y. Nakato, Z. Phys. Chem. 212 (1999) 99.
[21] K. Nakato, S. Takabayashi, A. Imanishi, K. Murakoshi, Y. Nakato, Sol. Energy Mater. Sol. Cells 83 (2004) 323.
[22] S. Takabayashi, A. Imanishi, Y. Nakato, Thin Solid Films, submitted.
[23] M.R. Linford, C.E.D. Chidsey, J. Am. Chem. Soc. 115 (1993) 12631.
[24] M.R. Linford, P. Fenter, P.M. Eisenberger, C.E.D. Chidsey, J. Am. Chem. Soc. 117 (1995) 3145.
[25] A. Bansal, X.L. Li, I. Lauermann, N.S. Lewis, S.I. Yi, W.H. Weinberg, J. Am. Chem. Soc. 118 (1996) 7225.
[26] M.M. Sung, G.J. Kluth, O.W. Yauw, R. Maboudian, Langmuir 13 (1997) 6164.
[27] J.M. Buriak, Chem. Commun. (1999) 1051.
[28] R.L. Cicero, M.R. Linford, C.E.D. Chidsey, Langmuir 16 (2000) 5688.
[29] T. Okubo, H. Tsuchiya, M. Sadakata, T. Yasuda, K. Tanaka, Appl. Surf. Sci. 171 (2001) 252.
[30] J.M. Buriak, Chem. Rev. 102 (2002) 1271.
[31] W.J. Royea, A. Juang, N.S. Lewis, Appl. Phys. Lett. 77 (2000) 1988.
[32] A. Bansal, N.S. Lewis, J. Phys. Chem. B 102 (1998) 4058.
[33] J. Cheng, D.B. Robinson, R.L. Cicero, T. Eberspacher, C.J. Barrelet, C.E.D. Chidsey, J. Phys. Chem. B 105 (2001) 10900.
[34] A. Bansal, N.S. Lewis, J. Phys. Chem. B 102 (1998) 1067.
[35] J. Terry, M.R. Linford, C. Wigren, R.Y. Cao, P. Pianetta, C.E.D. Chidsey, J. Appl. Phys. 85 (1999) 213.
[36] F.J. Himpsel, F.R. McFeely, A. Talebibrahimi, J.A. Yarmoff, G. Hollinger, Phys. Rev. B 38 (1988) 6084.
[37] T. Kisumi, A. Tsujiko, K. Murakoshi, Y. Nakato, J. Electroanal. Chem. 545 (2003) 99.
[38] R. Nakamura, Y. Nakato, J. Am. Chem. Soc. 126 (2004) 1290.